Crater Formation and Damage Optimisation on Soda-Lime Glass for LIBS Analysis

Patrik Gádoros*, Imre Péczeli, László Kocsányi, and Péter Richter

Department of Atomic Physics, Institute of Physics, Budapest University of Technology and Economics, Műegyetem rkp. 3, H-1111 Budapest, Hungary
**Corresponding author's e-mail: gadoros.patrik@ttk.bme.hu*

This paper gives an insight to formation of ablation craters on float glass samples due to irradiation by high energetic nanosecond laser pulses and its optimisation for laser-induced breakdown spectroscopy (LIBS) analysis. Use of such lasers is less common for material processing, therefore ablation and eventual degradation of the samples has not been in the focus technical studies. Meanwhile high energy pulses can be optimal for certain applications, such as LIBS. Here the properties of ablation craters on common float glass samples after high energetic laser pulse irradiation were investigated. LIBS spectra were obtained and their quality was compared against the irradiation parameters such as wavelength and focusing conditions. It was found that these have a significant effect on crater formation, but parameters can be set to allow ablation without major degradation of the sample.

DOI: 10.2961/jlmn.2023.01.2009
Keywords: ablation crater, glass, laser-induced breakdown spectroscopy (LIBS), nanosecond laser, laser-induced damage

1. Introduction

The size, shape and quality of laser craters and edges are critical features of both laser material processing and laser-based analysis techniques. High quality surface finish, chip-free cut edges and speed of material processing makes laser cutting ,drilling and engraving competitive with conventional material processing in spite of the high initial investment [1], while the decreased need of post processing reduces production costs significantly [2–3]. On the other hand, laser based analysis (e.g. laser-induced breakdown spectroscopy, LIBS) is often applied to sensitive objects such as artworks [4–5] The presence or absence of visible craters and micro-cracks significantly influences the visual and mechanical properties of the sample after analysis.

Many laser-based techniques are used in industrial practice to separate glass sheets, being the most customary the laser scribe and break technique. The cut surface is marked by a narrow groove or partially penetrating holes created by laser, then a mechanical force is applied on the workpiece. [6] Developments of this method aim the improvement of process capabilities regarding both scribe and break stages. [7–10] Controlled fracture technique is based on the laser-induced thermal-crack propagation (LITP). [11] By absorption of the laser radiation an uneven temperature field is generated within the material. If this stress exceeds the yield strength of the material, a crack will propagate towards it. [11] Since the heat stress itself is highly concentrated, the resulting surface is of good quality, and generally no post processing is required. Deep penetration makes laser radiation an excellent tool for separation of thick glass sheets.[12]

Creating grooves and holes on glass surface by leaser is a well-studied field. Beyond direct ablation with the laser beam there are many techniques that apply laser induced plasma to etch the glass surface. [13–18] The common within these approaches is that they utilize a laser wavelength that the workpiece is highly transparent to, and apply an absorbing target or surface layer on the workpiece. While there is minimal interaction between glass material and laser radiation, a microplasma is ignited on the target, and the surface modification of the workpiece is done by the interaction with the plasma. The most well-known techniques based on this principle are laser-induced plasma-assisted ablation (LIPAA) and laser-induced backside etching (LIBE). [19–21] Most important advantages are the improved control of the material removal, the decreased heat affected zone and the possibility of microcrack-free machining. [22–24] Chemical alteration of the surface is quite typical side effect of these techniques. It is mostly unwanted, but can be utilized for certain applications. [25–27]

For analysis purposes an innovative and promising tool using high energetic short laser pulses is laser-induced breakdown spectroscopy (LIBS). The laser radiation is focused on the sample surface to create microplasma from a small amount of the sample material, and the optical emission of this plasma is used to analyse the composition of the sample. [28–29] Here the analysis is the purpose, while the ablation is a collateral effect, which is in most cases considered as harmful, since leads to the degradation of the sample. Nonetheless there are many examples of connecting LIBS and laser micromachining and do analysis and processing in parallel. [30–31] There are encouraging results also with standalone LIBS on glass samples. They range from identification of archeologic or forensic glass fragments of unknown origin [32–35] and analysing corrosion layers on glass artefacts to monitoring of glass melting process and control glass processing. [36–41] Quantitative LIBS analysis can also be done on glass

samples both with calibration based and calibration free approach. [42–45] Our recent studies showed, that LIBS is an optimal tool for quantification of lithium (and possibly other light elements) in glass, which is difficult with actual analysis methods of silicate industry. [46]

The common drawback of all the aforementioned analysis techniques is the risk of chip and microcrack formation. Any surface flaw may initiate a crack and fracture the glass object when it is under heat or mechanical stress even due to normal use. [41–47] Microcracks belong to the most evident failure cause of this type, since they can compromise the structural strength of the material and serve as accumulation points of residual stress. [48–50] Crater morphology and crack formation – both intended and unintended – due to and pico- and femtosecond laser irradiation is technically quite well studied. [51–52] Meanwhile there is much less systematic analysis of the same phenomena when using high energetic nanosecond laser, although the risk of unwanted surface alteration is much higher in this case.

Furthermore, optimization of laser irradiation parameters is not simple. Many variables occur and a range of different physical phenomena have to be considered, some of them are quite complex on their own. These are, among others, thermal diffusion, ablation, plasma formation, plasma - target and plasma – laser beam interactions. The parameters to optimize include wavelength, focusing conditions, laser energy, scanning speed and number of passes. [53–56]

The target of this study is to discuss crater morphology and damage patterns in correlation with irradiation parameters. With suitable settings it will be possible to do LIBS analysis of commercial glassware and eventually perform laser cleaning and machining in parallel with the analysis. The criteria of such parameters require the absence of fractures, cracks and diffuse damage patterns, which would prevent normal use of the analysed piece. It is also necessary, that such features do not appear even after many consecutive laser shots to the same point.

2. Experimental

The experimental system was based on a Quantel Brilliant Q-switched Nd:YAG laser with frequency doubler and tripler modules (1064 nm, 532 nm and 355 nm), the energy of the pulses are 360 mJ, 180 mJ and 90 mJ respectively with the half width of 3.2 ns. The repetition rate was 20 Hz. The laser pulses were focused by a single quartz lens of 40.6 mm, 41.9 mm, and 43 mm focal length on the 3 wavelengths respectively. The shift of focal length is due to the dispersion of the quartz material of the lens. With the beam diameter of 5mm, the depth of focus (DOF) values 0.16 mm for 1064 nm wavelength, 0.08 mm for 532 nm and 0.05mm for 355 nm.

The light emitted by the plasma was gathered by a collector / collimator optics and led through fibre optics to the Mechelle-5000 echelle spectrograph equipped by an iStar i-734 ICCD camera. [Fig. 1] Settings of 2 μs delay and 5 μs acquisition times were used.

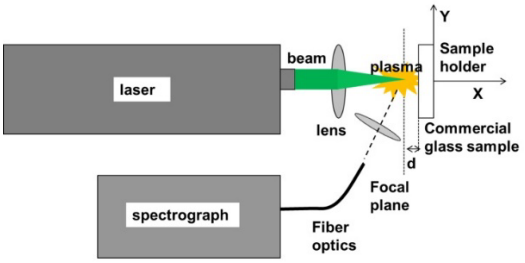

Fig. 1 Experimental setup

The samples were commercial soda-lime window glass pieces of dimensions 50x30x5 mm. The transparency was highly varying in the range of the excitation wavelength. [Fig. 2]

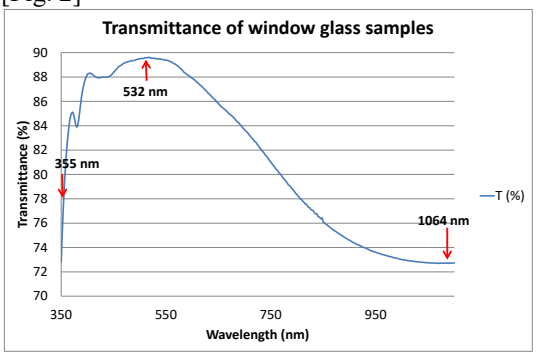

Fig. 2 Transmittance of the samples as a function of wavelength (the irradiation wavelengths are marked)

The laser pulses were focused in front of the sample surface (d=+1 mm), directly onto the surface (d=0mm) and below the surface into the bulk of the sample (d=-1 mm), which exceed considerably the DOF values. [Fig. 1] 1 to 100 shots were accumulated at one point of the sample to investigate the escalation of the damage with the increasing number of pulses. The ablated surfaces were qualified by optical microscopy (Olympus BX51 microscope equipped with DP72 camera) and optical profilometry (Bruker Contour GT-K0X). The heat affected zones were observed on the microscope images, the spot sizes were calculated from the focusing conditions. For the laser fluence the laser pulse energy and the (calculated) spot size was considered. The damage was later correlated to the LIBS spectra gained during the experiments.

3. Results and discussion

The observed damage patterns are those of brittle materials. In many cases there are clear ablation craters with material deposits around, that is the result of a well-controlled material removal process. Besides this effect far less controlled degradation of the samples can be observed due to overheating. It can be described by 3 basic patterns and their combinations: microcracks appear around the irradiation region, conchoidal fractures indicate the removal of bulky pieces, and diffuse internal damage show uncontrolled spread of thermal stress within the material. [Fig. 3]

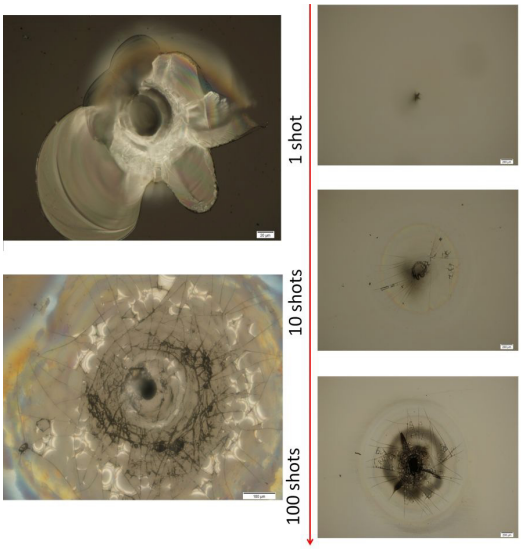

Fig. 3 Typical damage patterns observed; left top: conchoidal fracture (λ=355 nm, d=0 mm, 1 shot), left bottom: microcracks (λ=1064 nm, d=0 mm, 100 shots), right: diffuse internal damage, which propagates to the surfaces with the increasing number of shots (λ=1064 nm, d=-3 mm, 1, 10 and 100 shots corresponding).

These damage patterns conform to expectation. Microcracks and conchoidal fractures can be attributed to mechanical stress caused by local overheating of the sample in the focal volume. Meanwhile diffuse damage is most likely to have been caused by absorption of stray laser radiation outside the focal volume, still exceeding the yield strength of the material. Increasing the number of laser pulses, internal damage is prone to progress towards the sample surfaces. Focusing directly onto the surface results in the highest incident beam intensity, most powerful local heating and therefore highest heat stress. It leads consequently to an increased risk of creating cracks and fractures. [Fig. 4 and Table 1]

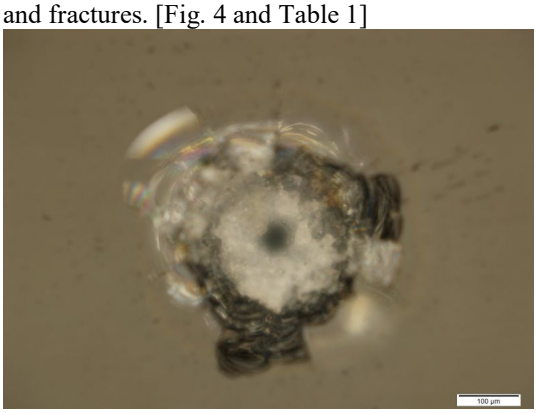

Fig. 4 λ=532 nm, d=0 mm, 10 shots, overheating of the sample is apparent

Table 1 Damage patterns after direct focusing of the laser beam. At all wavelengths and number of laser shots (except for 532 nm 1 shot) fractures and microcracks appear due to heat stress. Large heat affected zones (HAZ) are also observable [**Fig. 5**].

Wavelength	No. of shots	crater diameter (μm)	spot diameter (calculated, μm)	Laser fluence (J/cm^2)	diameter HAZ (mm)	damage pattern summary
1064 nm	1	not recognizable	12	3,E+05		conchoidal fracture 60x40μm
	10	40	12	3,E+05	0.8	HAZ covered by debris, microcracks of 0.2mm, 0.14mm circular surface clear around the crater
	100	40	12	3,E+05	1	0.8mm circular surface around the crater with many cracks and conchoidal fractures
532 nm	1	20	6	6,E+05	0.32	Nothing particular
	10	40	6	6,E+05	0.4	conchoidal fracture diameter 0.4mm
	100	300	6	6,E+05	2.6	conchoidal fracture 0.8mm diameter, radial cracks 0.7mm length, debris over the HAZ
355 nm	1	60	4	7,E+05	0.5	0.26x0.2mm conchoidal fracture
	10	60	4	7,E+05	2.7	diameter 3mm conchoidal fracture
	100	250	4	7,E+05	2.7	diameter 3.5mm conchoidal fractrue

This hazard may be reduced by defocusing the laser beam. However, in case of focusing below the surface, a shockwave is generated in the bulk material causing mechanical stress in quite an unfavourable way. Not only the ablation crater is prone to be deeper, meaning more material ablated, but a plasma shockwave maybe initiated inside the sample causing severe cracks and fractures. [Fig. 5] This entire problem can be avoided by focusing in front of the surface. In this way the plasma is generated in the air, thus internal damage of the sample can be minimized. Meanwhile the irradiated area is greater, than in case of focusing directly onto the surface causing more advantageous heating, reducing risk of cracks and fractures. [Fig. 6] In most cases the heat affected zone tends to decrease substantially when focusing in front of the sample. [Table 2]

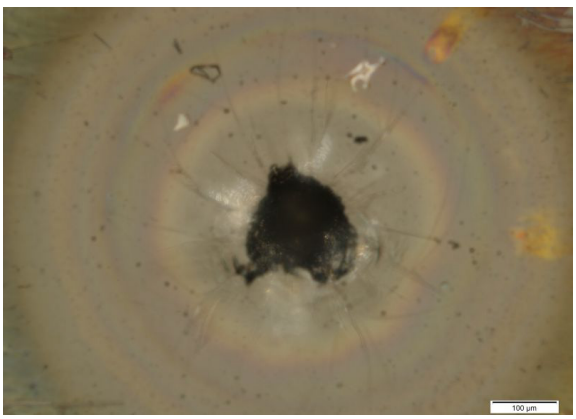

Fig. 5 λ=532 nm, d=-1 mm, 10 shots, the material expanding from inside caused extensive damage. One can observe the heat affected zone (HAZ), i.e., the large circular halo due to heat induced refractive index changes.

Table 2 Damage patterns after 100 consecutive laser shots – dependence of wavelength and defocusing

Wavelength	defocusing (mm)	crater diameter (μm)	spot diameter (calculated, μm)	laser fluence (J/cm2)	diameter HAZ (mm)	Conchoidal fracture	Microcracks
1064 nm	0	40	12	3,E+05	1	none	0.8 mm surface around the crater
	1	60	125	3,E+03	1	none	0.2 mm radial
	-1	150	125	3,E+03	3	none	1.5 mm surface around the crater
532 nm	0	300	6	6,E+05	2.6	0.8 mm	radial 0.7 mm length
	1	200	125	1,E+03	1	none	none
	-1	200	125	1,E+03	1.8	0.7 mm	0.2 mm long
355 nm	0	250	4	7,E+05	2.7	3.5 mm	not observable
	1	400	125	7,E+02	0.9	none	0.4 mm long
	-1	300	125	7,E+02	1.5	0.8 mm	0.6 mm long

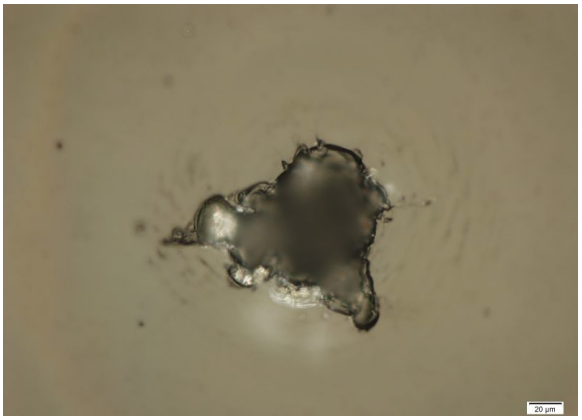

Fig. 6 λ=532 nm, d=+1 mm, 10 shots, due to favourable sample heating and minimal absorption of stray light the damage is limited to the ablation crater and therefor kept better under control

Wavelength has also a strong impact on the ablation process through plasma shielding and energy coupling [43], which influence the total amount of energy passed over to the sample. Furthermore, the damage pattern is strongly dependent on the spatial distribution of the absorbed energy, which also has a wavelength-factor due to the varying transmittance of the sample. In case of 355nm and 1064nm the absorption of stray radiation should be taken into account. 1064nm (with the highest absorption rate) is especially prone to cause some additional damage outside the focal volume [Fig. 7], while at 355nm this effect is less significant, but still a substantial damage can be expected at the surface. [Fig. 8] At 532nm this effect is minor resulting in a much better controlled damage pattern. [Fig. 6]

Fig. 7 λ=1064 nm, d=+1 mm, 100 shots, overheating the sample surface affects large area

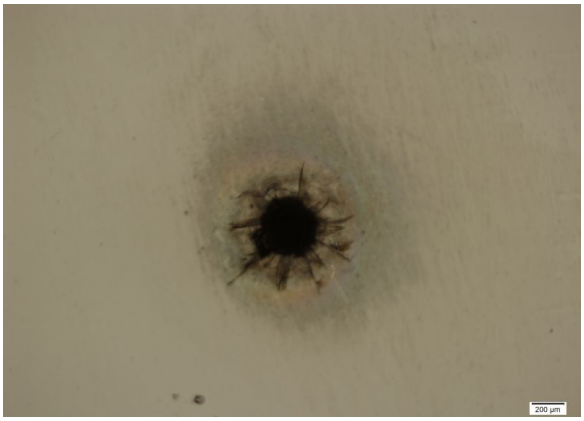

Fig. 8 λ=355 nm, d=+1 mm, 100 shots, absorption of stray laser radiation caused extensive damage

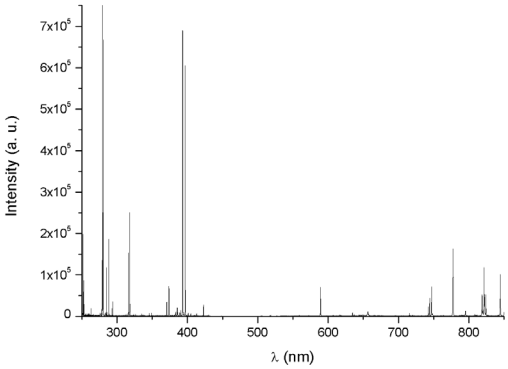

Fig. 9 A typical LIBS spectrum obtained during the experiment. Settings were: λ=1064 nm laser wavelength, 100 shots and d=+1 mm defocusing 2μs delay and 5 μs acquisition times

If we consider the capability of material analysis, this way of reducing the damage can have its' toll on the LIBS signal (**Fig. *9***) quality. Visible irradiation has been reported as suboptimal from the point of energy coupling and plasma shielding. [43] Focusing in front of the surface also causes more plasma heating and less energy transmitted to the sample. Excited components of the air (e. g. Nitrogen) become more dominant in the emitted LIBS signal, meanwhile slight decrease in the spectral line intensities of the analytes (e. g. Silicon) can be observed. [Fig. 10] As a result, uncertainty of the signal intensities is slightly higher [Fig. 11], thus the reproducibility is somewhat inferior to that at some other wavelengths or focusing positions.

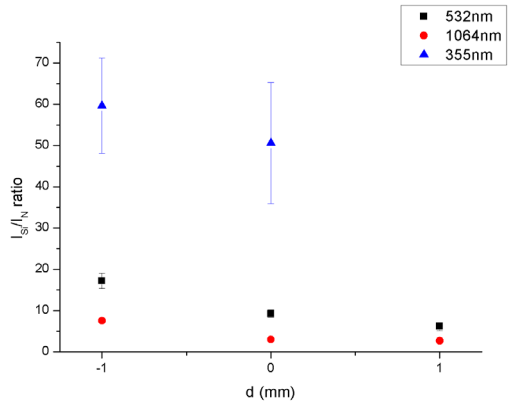

Fig. 10 Intensity ratio of Si I (288.2 nm) and N I (746.8 nm) peaks as a function of focus position at 1064 nm, 532 nm and 355 nm. In all cases, the signal of nitrogen becomes more significant if the focus is moved out of the sample.

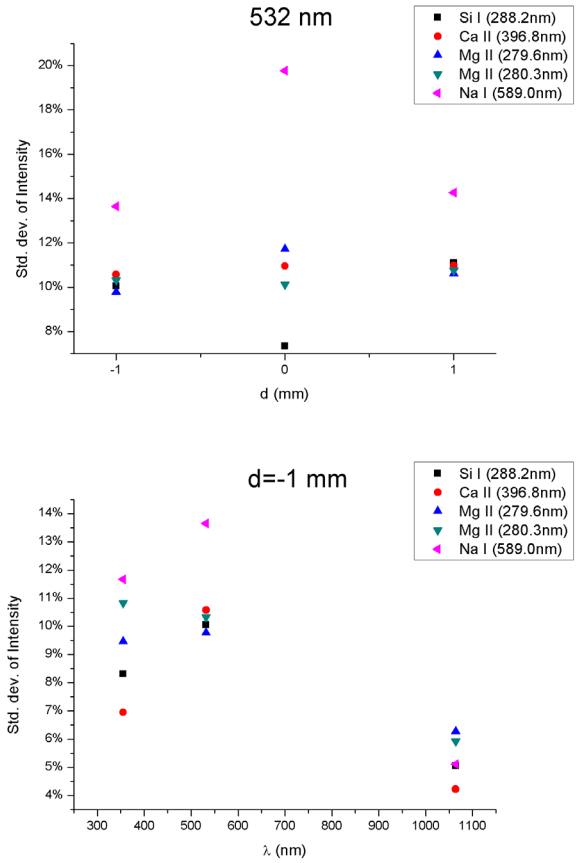

Fig. 11 Standard deviation of some signal intensities at different focal positions and wavelengths

All of the wavelengths and focusing conditions proved to suitable for LIBS analysis in the means of producing clear and assessable spectra. Best analysis capabilities, however, can be achieved by high signal to noise ratio and low relative standard deviation of spectral line intensities. [Fig. 12] maps the settings according to these quality markers, advancing to the right bottom of the image, the signal quality increases. Optimal setting for LIBS analysis is therefore 1064 nm laser wavelength and -1 mm defocusing. It is necessary to note that the extensive degradation of the sample (many microcracks and large HAZ) [**Table *2***] makes this setting not suitable for analysis of precious samples.

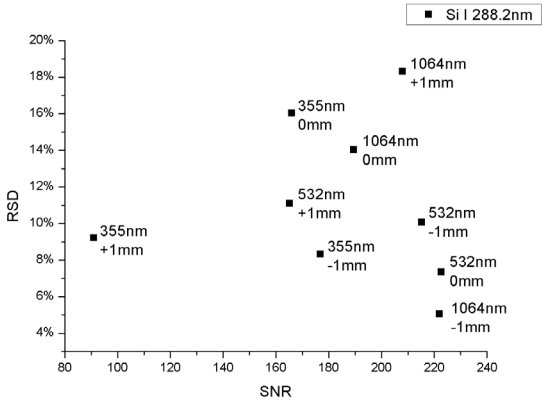

Fig. 12 Relative standard deviation (RSD) and signal to noise ratio (SNR) of Si I 288.2nm spectral line intensity. Optimal settings for LIBS analysis purpose are high SNR and low RSD.

4. Conclusion

All of the laser wavelengths and focusing conditions applied in the experiment proved to be suitable for LIBS analysis. There were, however, considerable differences in spectral quality and sample degradation. If microdestructive property of LIBS needs not to be exploited, most advised is focusing a 1064 nm laser beam below the sample surface (d=-1 mm). But this is no way the optimal setting for analysis of valuable samples, since extensive damage may occur.

Mechanical and optical degradation of the sample has proven minimal, when the high energy laser pulses were focused slightly in front of the sample and a wavelength was used where the sample is highly transparent, namely d=+1 mm and 532 nm. [Fig. 13] These settings could ensure a favourable distribution of the absorbed energy preventing cracks and fractures of the glass material. With an increasing number of shots both the diameter and the depth of the ablation crater increased, but no damage apart from it occurred. [Fig. 14] The actual number of laser pulses determine the size of the crater, but microcrack free ablation can be achieved by focusing the laser beam in front of the target surface.

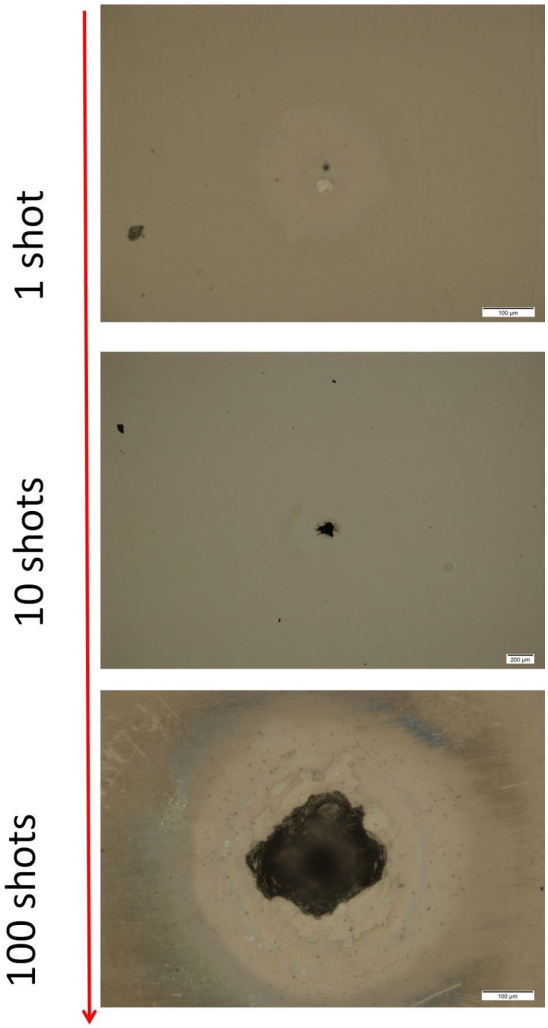

Fig. 13 Most robust setting is 532 nm irradiation focused in front of the sample (with 1mm in this experiment). The dimensions of the ablation crater increase with the number of shots, but the damage remains well controlled.

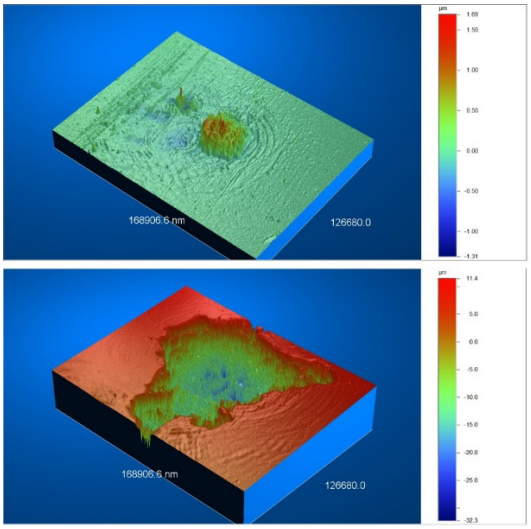

Fig. 14 3D profiles of the damage after measurement with the recommended settings, top: 1 shot, bottom: 10 shots

Acknowledgements

This research was funded by the National Research, Development, and Innovation Fund of Hungary under Grant TKP2021-NVA-02.

References

[1] S. Nikumb, Q. Chen, C. Li, H. Reshef, H. Y. Zheng, H. Qiu, and D. Low: Thin Solid Films, 477, (2005) 216.
[2] C. Ungaro and A. Liu: Opt. Laser Technol., 144, (2021) 107398.
[3] C. Ungaro, N. Kaliteevskiy, P. Sterlingov, V. V. Ivanov, A. Boh Ruffin, R. J. Terbrueggen, and N. Savidis: Appl. Opt., 60, (2021) 714.
[4] V. Detalle and X. Bai: Spectrochim. Acta B, 191, (2022) 106407.
[5] J. P. Dudeja: Lasers Eng., 48, (2021) 1.
[6] C. H. Tsai and B. C. Lin: Int. J. Adv. Manuf., 32, (2007) 1155.
[7] Y. Z. Wang and J. Lin: Opt. Laser Technol., 39, (2007) 892.
[8] Y. L. Kuo and J. Lin: Opt. Lasers Eng., 46, (2008) 388.
[9] S. Nisar, M. A. Sheikh, L. Li, and S. Safdar: Opt. Laser Technol., 41, (2009) 318.
[10] J. Dudutis, R. Stonys, G. Račiukaitis, and P. Gečys: Opt. Laser Technol., 111, (2019) 331.
[11] C. Zhao, H. Zhang, and Y. Wang: Opt. Lasers Eng., 63, (2014) 43.
[12] S. Butkus, D. Paipulas, R. Sirutkaitis, E. Gaižauskas, and V. Sirutkaitis: J. Laser Micro Nanoeng., 9, (2014) 213.
[13] M. H. Hong, K. Sugioka, D. J. Wu, L. L. Wong, Y. Lu, K. Midorikawa, and T. C. Chong: Photon Process. Microelectron. Photon., 4637, (2002) 270.
[14] M. Hong, K. Sugioka, D. J. Wu, L. L. Wong, Y. Lu, K. Midorikawa, and T. C. Chong,. Proc. SPIE, 4595, (2001) 138.
[15] G. K. Kostyuk, M. M. Sergeev, R. A. Zakoldaev, and E. B. Yakovlev: Opt. Lasers Eng., 68, (2015) 16.
[16] P. Lorenz, M. Ehrhardt, and K. Zimmer: Appl. Surf. Sci., 258, (2012) 9742.
[17] D. Nieto, T. Delgado, and M. T. Flores-Arias: Opt. Lasers Eng., 63, (2014) 11.
[18] T. U. Rahman, Z. U. Rehman, S. Ullah, H. Qayyum, B. Shafique, R. Ali, U. Liaqat, A. H. Dogar, and A. Qayyum: Opt. Laser Technol., 120, (2019) 105768.
[19] C. Pan, K. Chen, B. Liu, L. Ren, J. Wang, Q. Hu, L. Liang, J. Zhou, and L. Jiang: J. Mater Process. Technol., 240, (2017) 314.
[20] J. Long, J. Li, M. Li, and X. Xie: Surf. Coat., 374, (2019) 338.
[21] J. Zhang, K. Sugioka, and K. Midorikawa: Opt. Lett., 23, (1998) 1486.
[22] X. Ding, Y. Kawaguchi, T. Sato, A. Narazaki, R. Kurosaki, and H. Niino: J. Photochem. Photobiol., 166, (2004) 129.
[23] Y. Kawaguchi, T. Sato, A. Narazaki, R. Kurosaki, and H. Niino: J. Photochem. Photobiol., 182, (2006) 319.

[24] K. K. Kwon, H. Kim, T. Kim, and C. N. Chu: J. Mater Process. Technol., 278, (2020) 116505.
[25] Y. Xia, X. Jing, D. Zhang, F. Wang, S. H. I. Jaffery, and H. Li: Infrared Phys. Technol., 115, (2021) 103737.
[26] C. Zhang, Y. Yu, Y. Cao, X. Wei, S. Su, and W. Liu: Opt. Laser Technol., 138, (2021) 106849.
[27] S. Xu, B. Liu, C. Pan, L. Ren, B. Tang, Q. Hu, and L. Jiang: J. Mater Process. Technol., 247, (2017) 204.
[28] S. M. Clegg, R. B. Anderson, and N. Melikechi: Remote Compos. Anal., (Cambridge University Press, 2019) p.168.
[29] S. K. Hussain Shah, J. Iqbal, P. Ahmad, M. U. Khandaker, S. Haq, and M. Naeem: Radiat. Phys. Chem., 170, (2020) 108666.
[30] D. Diego-Vallejo, M. Schwagmeier, D. Ashkenasi, G. Illing, and H. J. Eich-Ler: J. Laser Micro Nanoeng., 6, (2011) 146.
[31] J. Skruibis, O. Balachninaite, S. Butkus, V. Vaicaitis, and V. Sirutkaitis: Opt. Laser Technol., 111, (2019) 295.
[32] C. M. Bridge, J. Powell, K. L. Steele, M. Williams, J. M. MacInnis, and M. E. Sigman: Appl. Spectrosc., 60, (2006) 1181.
[33] E. M. Rodriguez-Celis, I. B. Gornushkin, U. M. Heitmann, J. R. Almirall, B. W. Smith, J. D. Winefordner, and N. Omenetto: Anal. Bioanal. Chem., 391, (2008) 1961.
[34] B. E. Naes, S. Umpierrez, S. Ryland, C. Barnett, and J. R. Almirall: Spectrochim. Acta B, 63, (2008) 1145.
[35] K. Müller and H. Stege: Archaeometry, 45, (2003) 421.
[36] N. Carmona, M. Oujja, E. Rebollar, H. Römich, and M. Castillejo: Spectrochim. Acta B, 60, (2005) 1155.
[37] U. Panne, R. E. Neuhauser, C. Haisch, H. Fink, and R. Niessner: Appl. Spectrosc., 56, (2002) 375.
[38] U. Panne, M. Clara, C. Haisch, and R. Niessner: Spectrochim. Acta B, 53, (1998) 1969.
[39] U. Panne, C. Haisch, M. Clara, and R. Niessner: Spectrochim Acta B, 53, (1998) 1957.
[40] B. Lal, F.-Y. Yueh, and J. P. Singh: Appl. Opt., 44, (2005) 3668.
[41] A.-M. Matiaske, I. B. Gornushkin, and U. Panne: Anal. Bioanal. Chem., 402, (2012) 2597.
[42] E. M. Cahoon and J. R. Almirall: Appl. Opt., 49, (2010) 49.
[43] K. Loebe, A. Uhl, and H. Lucht: Appl. Opt., 42, (2003) 6166.
[44] V. S. Burakov, V. V Kiris, P. A. Naumenkov, and S. N. Raikov: J. Appl. Spectrosc., 71, (2004) 740.
[45] C. Gerhard, J. Hermann, L. Mercadier, L. Loewenthal, E. Axente, C. R. Luculescu, T. Sarnet, M. Sentis, and W. Viöl: Spectrochim. Acta B, 101, (2014) 32.
[46] P. Gádoros, T. Váczi, L. Himics, R. Holomb, R. Bolla, M. Veres, and L. Kocsányi: J. Non Cryst. Solids., 553, (2021) 14.
[47] K. Maeda, K. Akatsuka, and A. Yasumori: Ceram. Int., 47, (2021) 8728.
[48] T. Rouxel and S. Yoshida: J. Am. Ceram., 100, (2017) 4374.
[49] A. K. Varshneya: Int. J. Appl. Glass. Sci., 9, (2018) 140.
[50] K. Maeda and Y. Nakao: J. Soc. Inf. Disp., 11, (2003) 481.
[51] M. Sun, U. Eppelt, C. Hartmann, W. Schulz, J. Zhu, and Z. Lin: Opt. Laser Technol., 80, (2016) 227.
[52] T. U. Rahman, Z. U. Rehman, S. Ullah, H. Qayyum, B. Shafique, R. Ali, U. Liaqat, A. H. Dogar, and A. Qayyum: Opt. Laser Technol., 120, (2019) 105768.
[53] V. S. Rymkevich, M. M. Sergeev, and R. A. Zakoldaev: J. Mater. Process. Technol., 292, (2021) 117061.
[54] C. Barnett, E. Cahoon, and J. R. Almirall: Spectrochim. Acta B, 63, (2008) 1016.
[55] S. Xiong, R. Wang, and H. Tao: J. Eur. Ceram. Soc., 41, (2021) 5990.
[56] E. Bulushev, V. Bessmeltsev, A. Dostovalov, N. Goloshevsky, and A. Wolf: Opt. Lasers Eng., 79, (2016) 39–47.

(Received: October 1, 2022, Accepted: April 28, 2023)